IJE TRANSACTIONS C: Aspects Vol. 36 No. 12, (December 2023) 2161-2168

International Journal of Engineering

Journal Homepage: www.ije.ir

Development of a Wideband Bi-layered Mantle-Cloak for Perfect Electric Conductor Cylindrical Objects under Obliquely Incident Plane Wave

A. Moosaei, M. H. Neshati*

Department of Electrical Engineering, Faculty of Engineering, Ferdowsi University of Mashhad, Mashhad, Iran

PAPER INFO

Paper history:
Received 17 May 2023
Received in revised form 04 September 2023
Accepted 09 September 2023

Keywords:
Mantele Cloak
Electromagnetic Invisibility
Metasurface
Oblique Incidence

ABSTRACT

This paper presents a mantle cloak structure to provide a wideband capability to hide a metallic cylinder over a broad span of angles of obliquely impinging plane waves. A bi-layered dielectric structure and a sheet of metasurface are used to enclose the object to be hidden. At first, the scattered field, including co- and cross-polarized components, is analytically formulated using circumferential waves for a multi-layer wrap around the cylinder. A tensor description is also applied to model the impedance of the metasurface for TE and TM waves. Then, a metasurface made of rectangular patches is considered, and its related parameters are optimized to hide a perfect electric conductor (PEC) cylinder. Moreover, a double-layered mantle cloak is presented and numerically investigated using a software package to enhance its cloaking bandwidth. The numerical results show that the clocking bandwidth is enhanced by up to 33% compared to that of a single-layered structure.

***doi**: 10.5829/ije.2023.36.12c.04*

1. INTRODUCTION

New advances in metamaterial technology propose the feasibility of electromagnetics invisibility, which mainly relies on the complex interaction between waves and artificial materials [1-3]. To this end, Pendry et al. [4] introduced the Coordinate Transform (CT) method, considered one of the most effective techniques to achieve invisibility [5], which relies on the concept of the curving electromagnetic waves around the object performed by employing a special coating to create an enclosed environment, which ensures that the illuminated waves move around the object to avoid reflecting, interpreting the interior space of the container as virtually invisible. By this method, an ideal conversion-based coating could completely separate the coated object, making it appear that the coating and inner area do not exist in terms of electromagnetic properties [6].

As of late, there have been significant improvements in making metamaterials. In this regard, experimental evidence has validated the application of the CT technique to microwave bands. Numerous efforts have been made to apply this method to visible light frequencies [1, 7, 8]. Plasmonic cloaking is another helpful technique to achieve invisibility using the property of scattering elimination using metamaterials with a low electrical permeability coefficient [9-13] which creates an anti-phase scattering wave, reducing the scattered fields and eventually concealing the object.

Other unconventional techniques have been investigated in the literature in covering a sphere to be invisible. The limited size of the applied metamaterial coating results in an inherent need for a certain thickness. However, increasing the thickness of the layer is not suitable due to reducing bandwidth and increasing sensitivity. The plasmonic cloaking method requires thinner layers than the conversion-based approach and typically requires a finite thickness to function correctly [14-16].

A new masking technique based on the concept of mantle cloak has been proposed to address this issue by decreasing the Radar Cross Section (RCS) for various shaped objects, including planar, cylindrical, elliptical, and spheroidal objects at microwave and lower band of terahertz (THz) frequencies [14, 15, 17-20]. This

*Corresponding author email: *neshat@um.ac.ir* (M. H. Neshati)

Please cite this article as: A. Moosaei, M. H. Neshati, Development of a Wideband Bi-layered Mantle-Cloak for Perfect Electric Conductor Cylindrical Objects under Obliquely Incident Plane Wave, ***International Journal of Engineering, Transactions C: Aspects***, Vol. 36, No. 12, (2023), 2161-2168

technique relies on a patterned conductive thin surface coating, known as a metasurface, to diminish the scattered components appropriately. By calculating the parameters of the metasurface, an optimal surface reactance is obtained to effectively suppress the object's scattered fields, resulting in its invisibility.

Most published research on cylindrical objects focuses on obtaining cloaking for TE and TM plane waves illuminated perpendicular to the PEC cylinders. In contrast, electromagnetic cloaking in the case of obliquely illuminated waves is still a challenging topic, that demands further investigation [21]. Most investigations have examined the performance of isotropic mantle cloaks, designed to be inductive or capacitive in one or two dimensions. Nevertheless, in practical applications, reducing the scattered field by cylindrical objects with thicknesses comparable to the wavelength of the incident wave is often preferable. This reduction should be satisfied over a wide range of polarization states.

When an obliquely incident electromagnetic wave illuminates a PEC cylinder, coupling polarization occurs, leading to an increase in the total *RCS* of the structure, which is generally undesirable. In addition, the cloaking frequency range is slightly shifted, which is also a challenging task. It should be pointed out that while an obliquely incident wave exposes a bare PEC cylinder, the scattered fields are not coupled. In contrast, the cross-polarized coupling is introduced for a dielectric or coated PEC cylinder using dielectric layers [22]. As a result, scattering, and consequently acquiring invisibility is an exciting subject [23]. Moreover, covering these objects over a wide range of angles of the incident wave is another exciting issue due to existing of the cross-coupling.

In a few studies, graphene has been applied as a mantle-cloaked material for dielectric cylinders with low permittivity at lower frequencies of the tera-hertz band [24, 25]. Nonetheless, the authors facilitated their analytical explanation by bypassing the cross-polarized components of the scattered fields. This simplification is necessary due to the cylinder's small size and low permittivity. A comparable level of simplification was considered by Bilotti et al. [26]. Additionally, a single-layered mantle cloak, possessing specific surface reactance, simply suppresses one or, at most, a limited number of orders of the scattered field, whereas using multi-layered coating introduces a few benefits, including the ability to suppress higher orders of the scattered fields, facilitating multi-band and wideband invisibility. Moreover, the range of invisibility angle is widened, and more importantly, cloaking feasibility for TM and TE polarized waves.

In our previous study [21], we thoroughly addressed and validated the analytical formulation of the scattering issue for a metallic cylinder enlightened obliquely by TM and TE polarized wave. A single-layered mantle cloak is also designed and optimized to suppress the scattered components by considering the co- and cross-polarized terms.

In this paper, the preliminary step involves expressing the scattered fields concerning co- and cross-polarized components originating from the PEC cylinder coated with multiple layers of dielectric material and subjected to the oblique incidence of a plane wave. Afterward, a numerical study is accomplished using CST EM simulator [27] to evaluate the accuracy of the derived results for a bi-layered structure. Moreover, further investigations are directed to develop upon the findings for a bi-layered mantel cloak to lessen the *RCS* of the metallic cylinders over a wide frequency range.

2. SCATTERING FORMULATION

2. 1. Single-Layered Mantel Cloak Figure 1 shows a single-layered mantel cloak, in which a metallic cylinder with a radius of a is covered by a dielectric layer with a thickness of between a and a_d. In addition, a metasurface is positioned directly on top of the spacer. The mantle cloak impedance is formulated by a tensor consisting of off-diagonal terms, in which the cross-polarized components are considered. These factors are mathematically represented by Equation (1) to model the metasurface impedance.

$$Z_s = \begin{bmatrix} Z_s^{\mathrm{TM,TE}} & Z_s^{\mathrm{TM,TE}} \\ Z_s^{\mathrm{TM,TE}} & Z_s^{\mathrm{TM,TE}} \end{bmatrix}, \tag{1}$$

An oblique incident wave is illuminated on the cylinder by the angle of φ_i and inclination angle of θ_i as shown in Figure 1. For a TM wave, the cylindrical harmonics of the electric field are given by Equation (2) [28].

$$\begin{aligned} \mathbf{E}_i &= \mathbf{E}_1 e^{-j\mathbf{k}_i \cdot \mathbf{r}} \\ &= \mathbf{E}_1 e^{jk_1 \cos\theta_i z} \sum_{n=-\infty}^{\infty} j^n J_n(k_1 \rho \sin\theta_i) e^{jn(\varphi-\varphi_i)} \end{aligned} \tag{2}$$

Using Jacobi-Anger expansion [28], electric fields inside the dielectric layer and its associated cross-polarized

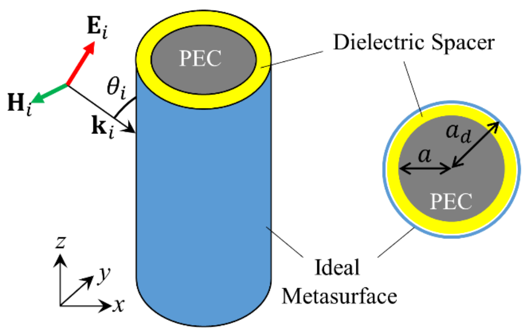

Figure 1. Single-layered mantel cloak using metasurface to cover the PEC cylinder illuminated obliquely by a plane wave

terms of the scattered fields are specified by Equations (3a) to (3c), in which $J_n(.)$ and Y_n (.) represent ordinary Bessel functions of the first and second kind in cylindrical coordinates, respectively. $H_n^{(2)}(\cdot)$ denotes the second kind of Hankel function, to articulate an outward-traveling cylindrical wave.

$$E_i^z = \sin\theta_i e^{jk_1\cos\theta_i z} \sum_{n=-\infty}^{\infty} j^n J_n(k_1 \sin\theta_i \rho e^{jn(\varphi-\varphi_i)} \tag{3a}$$

$$E_s^z = \sin\theta_i e^{jk_1\cos\theta_i z} \sum_{n=-\infty}^{\infty} A_n^{co} H_n^{(2)}(k_1 \sin\theta_i \rho) e^{jn(\varphi-\varphi_i)} \tag{3b}$$

$$E_d^z = \sin\theta_t e^{jk_2\cos\theta_t z} \sum_{n=-\infty}^{\infty} \left[C_n^{co} J_n(k_2 \sin\theta_t \rho) + D_n^{co} Y_n(k_2 \sin\theta_t \rho)\right] e^{jn(\varphi-\varphi_i)} \tag{3c}$$

Equations (4a) and (4b) also give the cross-polarized components.

$$H_s^z = \sin\theta_i e^{jk_1\cos\theta_i z} \sum_{n=-\infty}^{\infty} B_n^{cr} H_n^{(2)}(k_1 \sin\theta_i \rho) e^{jn(\varphi-\varphi_i)} \tag{4a}$$

$$H_d^z = \sin\theta_t e^{jk_2\cos\theta_t z} \sum_{n=-\infty}^{\infty} E_n^{cr} J_n(k_2 \sin\theta_t \rho) + F_n^{cr} Y_n(k_2 \sin\theta_t \rho)\Big] e^{jn(\varphi-\varphi_i)} \tag{4b}$$

Using impedance boundary conditions at the metasurface with a radius of $\rho = a_d$, the unknown coefficients of the mentioned equations are calculated. This is involved to satisfy the continuity of the tangential components of the electric fields. In addition, the discontinuity of the tangential terms of the magnetic field by the total induced current on the metasurface is the other condition. In addition, the continuity of the tangential components of electric and magnetic fields have to be satisfied on the planar surface, and the absence of tangential electric fields on the surface of the cylinder.

The σ_{2D}^{TM} of the structure is obtained by summation of the co- and cross-polarized terms of the scatted fields, calculated by the asymptotic forms of Hankel functions and their derivatives [22]. For a TM wave, σ_{2D}^{TM} is obtained using Equations (5a) to (5c).

$$\sigma_{2D}^{TM} = \sigma_{2D}^{TM,CO} + \sigma_{2D}^{TM,CR} \tag{5a}$$

$$\sigma_{2D}^{TM,CO} = \frac{4}{k_1 \sin\theta_i^2} \left| \sum_{n=-\infty}^{\infty} A_n^{co} j^n e^{jn(\varphi-\varphi_i)} \right|^2 \tag{5b}$$

$$\sigma_{2D}^{TE,CR} = \frac{4\eta_1^2}{k_1 \sin\theta_i^2} \left| \sum_{n=-\infty}^{\infty} B_n^{CR} j^{n+1} e^{jn(\varphi-\varphi_i)} \right|^2 \tag{5c}$$

2. 2. Multi-Layered Mantel Cloak To develop the concept of a mantle cloak using a multi-layered structure, the scattering formulation is extended for non-electrically small objects over a wide frequency range. In this instance, the focus is directed towards an arrangement featuring an infinitely extended cylinder of a radius of a, which is covered by N conformal anisotropic metasurfaces, which exhibit an effective surface impedance tensor equivalent to Z_S^1 and Z_S^N given by Equation (6a).

$$Z_S^i = \begin{bmatrix} Z_S^{\mathrm{TM,TM},i} & Z_S^{\mathrm{TM,TE},i} \\ Z_S^{\mathrm{TE,TM},i} & Z_S^{\mathrm{TE,TE},i} \end{bmatrix}, i = 1,2,\cdots N, \tag{6a}$$

The metasurfaces' radii are denoted by Equation (6b).

$$a_{d,i} = \gamma_i a, \quad i = 1,2,\cdots N, \tag{6b}$$

In addition, the object under consideration is subjected to an external obliquely incident plane wave, with the electric field oriented parallel to the cylinder axis, known as TM, or perpendicular to it, designated as TE wave. The electromagnetic formulation conducted in the case of mentioned scenario is comparable to that of the single-layered mantle cloak. The only difference is the existence of an additional spatial term (between two metasurfaces) in which the electric field E_z^d requires an accurate description. Equation (7a) is used for the co-polarized components.

$$E_d^z = \sum_{n=-\infty}^{\infty} e^{jn(\varphi-\varphi_i)} \times \begin{cases} \sin\theta_{t1} e^{jk_1 z\cos\theta_{t1}} \times \\ \left[C1_n^{co} J_n(k_1'\rho) + D1_n^{co} Y_n(k_1'\rho)\right], a < \rho < a_{d1} \\ \sin\theta_{tN} e^{jk_N z\cos\theta_{tN}} \times \\ \left[CN_n^{co} J_n(k_N'\rho) + DN_n^{co} Y_n(k_N'\rho)\right], a_{d(N-1)} < \rho < a_{dN} \end{cases} \tag{7a}$$

Moreover, Equation (7b) is given for the cross-polarization terms.

$$H_d^z = \sum_{n=-\infty}^{\infty} e^{jn(\varphi-\varphi_i)} \times \begin{cases} \sin\theta_{t1} e^{jk_1 z\cos\theta_{t1}} \times \\ \left[E1_n^{cr} J_n(k_1'\rho) + F1_n^{cr} Y_n(k_1'\rho)\right], a < \rho < a_{d1} \\ \sin\theta_{tN} e^{jk_N z\cos\theta_{tN}} \times \\ \left[EN_n^{cr} J_n(k_N'\rho) + FN_n^{cr} Y_n(k_N'\rho)\right], a_{d(N-1)} < \rho < a_{dN} \end{cases} \tag{7b}$$

Applying the boundary conditions at the surface between two adjacent layers, yields $4N$+2 mathematical statements. Therefore, ($4N$+2)×($4N$+2) equations are obtained, and its solution determines the unknown coefficients, including A_n^{co}, B_n^{cr}, Ci_n^{co}, Di_n^{co}, Ei_n^{cr} and Fi_n^{cr}.

2. 3. Bi-Layered Mantel Cloak As a specific example of a multi-layered mantel cloak, a bi-layered structure is considered in this section, which is shown in Figure 2. Considering a TM-polarized wave illuminates the object under investigation, the impinged, scattered, and transferred electric and magnetic fields are denoted by Equations (8a) to (8d).

$$E_i^z = \sin\theta_i e^{jk_1\cos\theta_i z} \sum_{n=-\infty}^{\infty} j^n J_n(k_1 \sin\theta_i \rho e^{jn(\varphi-\varphi_i)} \tag{8a}$$

$$E_s^z = \sin\theta_i e^{jk_1\cos\theta_i z} \sum_{n=-\infty}^{\infty} A_n^{co} H_n^{(2)}(k_1 \sin\theta_i \rho) e^{jn(\varphi-\varphi_i)} \tag{8b}$$

$$E_{d1}^z = \sin\theta_{t1} e^{jk_3\cos\theta_{t1} z} \sum_{n=-\infty}^{\infty} \left[C1_n^{co} J_n(k_3 \sin\theta_{t1}\rho) + D1_n^{co} Y_n(k_3 \sin\theta_{t1}\rho)\right] e^{jn(\varphi-\varphi_i)} \tag{8c}$$

$$E_{d2}^z = \sin\theta_{t2} e^{jk_2\cos\theta_{t2} z} \sum_{n=-\infty}^{\infty} \left[C2_n^{co} J_n(k_2 \sin\theta_{t2}\rho) + D2_n^{co} Y_n(k_2 \sin\theta_{t2}\rho)\right] e^{jn(\varphi-\varphi_i)} \tag{8d}$$

The cross-polarized terms are also provided by Equations (9a) to (9c).

$$H_s^z = \sin\theta_i e^{jk_1\cos\theta_i z} \sum_{n=-\infty}^{\infty} B_n^{cr} H_n^{(2)}(k_1 \sin\theta_i \rho) e^{jn(\varphi-\varphi_i)} \tag{9a}$$

$$H_{d1}^z = \sin\theta_{t1} e^{jk_3\cos\theta_{t1} z} \sum_{n=-\infty}^{\infty} E1_n^{cr} J_n(k_3 \sin\theta_{t1}\rho) + F1_n^{cr} Y_n(k_3 \sin\theta_{t1}\rho)\Big] e^{jn(\varphi-\varphi_i)} \tag{9b}$$

$$H_{d2}^z = \sin\theta_{t2} e^{jk_2\cos\theta_{t2} z} \sum_{n=-\infty}^{\infty} E2_n^{cr} J_n(k_2 \sin\theta_{t2}\rho) + F2_n^{cr} Y_n(k_3 \sin\theta_{t2}\rho)\Big] e^{jn(\varphi-\varphi_i)} \tag{9c}$$

It should be noted that using the duality theorem, the scattered fields for a TE plane wave are derived using the same method as that of the TM one [21]. Accordingly, ten equations are obtained, which can be solved by applying boundary conditions, leading to finding scattering coefficients at different boundaries. Then, using the obtained coefficients, including A_n^{co} and B_n^{cr}, the total *RCS* of the object is calculated.

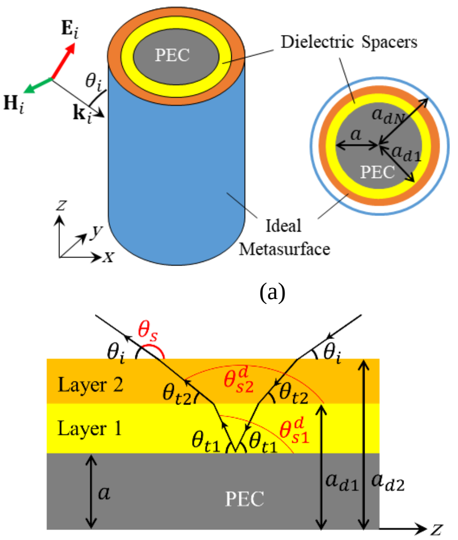

(b)

Figure 2. (a) bi-layered mantel cloak to invisible a dielectric-coated cylinder under oblique incidence wave, (b) side view and the definition of the incident and scattered angle

3. RESULTS AND DISCUSSION

3. 1. Single-layered Mantel Cloak

To design a single-layered cloak, a metallic cylinder is considered in our investigation with a length and radius of $10\lambda_o$ and $0.1\lambda_o$, respectively, and λ_o is the free space wavelength at 3 GHz. The cylinder is illuminated by an obliquely oriented TM wave at 3 GHz with $\theta_i = 60°$and the polarization plane is perpendicular to the propagation direction.

Figure 3 depicts the simulated scattering width contours versus chromaticity based on a relative radius of a_d/a and the vital metasurface impedance, X_S^{TM}, for the dielectric constant of $\varepsilon_r = 4$. Moreover, it can be concluded that $X_S^{TM} = -50\,\Omega$ is required to achieve minimum scattering width, $\sigma_{2D} \le -7$ dB, corresponding to the thickness of $a_d = 1.2a$. So, depending on the covering radius, obtaining the minimum scattering width for a cylinder at a specific value of the surface reactance, denoted by *Xs*, is feasible. The aforementioned minimum scattering width significantly reduces the object's visibility, thereby establishing cloaking effectiveness. Figure 4 shows the required impedance of the applied metasurface for the mentioned metallic cylinder, whereas the dielectric constant of the spacer is $\varepsilon_r = 4$ and its thickness is $a_d = 1.2a$. It shows the scattering width versus X_S^{TM} and X_S^{TE}, obtained by assuming $\sigma_{2D} \approx -7$ dB, which indicates $X_S^{TM} = -47\Omega$ and $X_S^{TE} = -17\,\Omega$.

3. 2. Bi-Layered Mantel Cloak

To evaluate the impact of the radius cylinder on the scattered fields, a TM

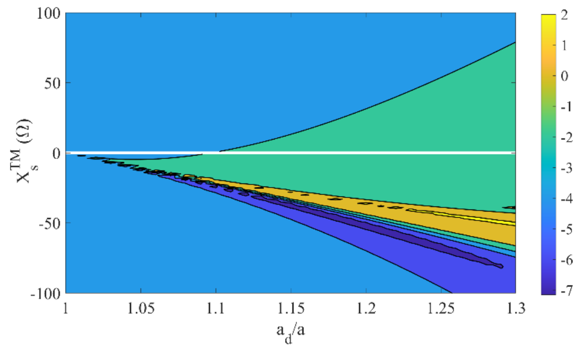

Figure 3. The surface impedance of metasurface for an obliquely incident TM wave and $\sigma_{2D} \approx -7$ dB versus relative radius of a_d/a

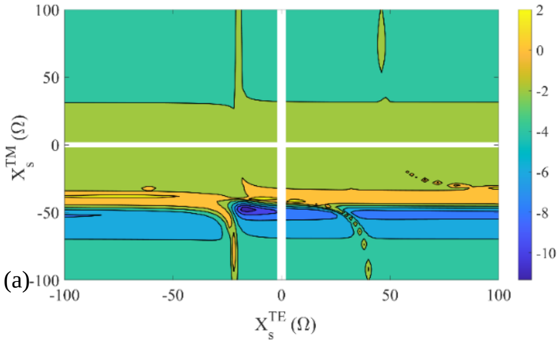

Figure 4. The required covering reactance of the metasurface for an oblique incident TM polarized wave on a dielectric-coated cylinder

wave at 3 GHz is obliquely illuminated by $\theta_i = 60°$ on a dielectric-coated metallic cylinder with relative permittivity of 15. Then, the magnitude of the co-polarized scattering coefficients A_n^{co}, in Equation (8b), are calculated. The results are illustrated in Figure 5 for two different cylinder radii of $a = 0.1\lambda_o$ and $a = \lambda_o$. The results confirm that for a PEC cylinder with a radius smaller than the operating wavelength, only the zeroth scattering mode contributes to the co-polarized scatter

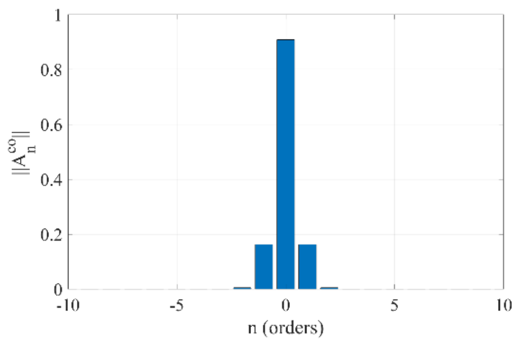

(a)

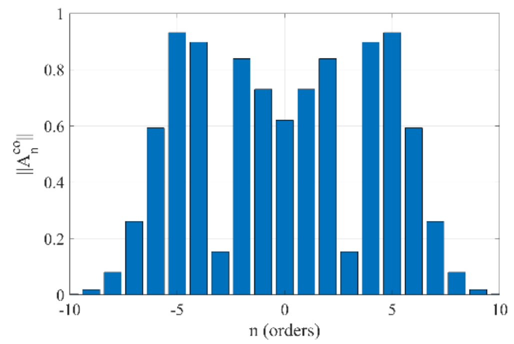

(b)

Figure 5. The radius-dependent scattering coefficients of a dielectric-covered metallic cylinder with relative permittivity of $\varepsilon_r = 15$ and cylinder radius of a) $a = 0.1\lambda_o$, b) $a = \lambda_o$.

fields, while for cylinders with a radius of nearly λ_o, free space wavelength, at least up to the eight order of the scattering modes affect the co-polarized terms.

Due to the ability of a metasurface to manipulate a single scattering mode, it is now possible to achieve cloaking for the objects that satisfy the quasi-static condition, in which the cylinder radius satisfies r ≤ λ_0 /10 [Ergin, #1]. As can be appreciated from Figure 5, depending on the covering radius, there exists the possibility to obtain a minimum scattering width for a cylinder at a specific magnitude of the surface reactance of the cloak, denoted by X_s. The minimum scattering width is linked to significantly reducing the object's visibility. Nonetheless, dielectric objects require a positive surface reactance, which is an inductive surface, while in the case of metallic objects, they require a sheet of capacitive reactance.

It is worth saying that the application of the single-layered mantle cloaking in reducing the total *RCS* is only limited to small radius cylinders relative to the operating free-space wavelength over a narrow bandwidth. However, for large objects multi-layered covering structure is proposed to widen available bandwidth [18].

Because the examination of metallic cylinders is significantly more pronounced when interacting with a TM wave in comparison with that of a TE one, in this paper, a TM wave at 3 GHz illuminates a limited length of a cylinder with a radius of $a = 0.1\lambda_o$ and a length of $L = \lambda_o$ at $\theta_i = 60°$ and the required mantle cloak is designed to obtain low total *RCS*.

As discussed in section II, using a single- or bi-layered dielectric covering with a dielectric constant of 4, which provides capacitive reactance, the required reactance are $X_S^{TM} = -23\,\Omega$ and $X_S^{TE} = -5\,\Omega$. To design the required metasurface providing the mentioned values of reactance, a quadrilateral capacitive patch is applied as shown in Figure 6. This structure provides two distinct periodicity parameters including D_z and D_φ, which are optimized to satisfy the required situation. Initially, Equation (10) is used to estimate X_S^{TM}, in which c and η_o represent light speed and inherent impedance of free space, respectively. Table 1 summarizes the optimal parameters of the single- and bi-layered designed mantle cloaks. In this regard, in our optimization process, initially, we assume to have geometrical parameters obtained from analytical formula. Then, we run the optimizer in CST MWS to achieve a minimum total RCS.

$$X_S^{TM} = \frac{\eta_o \pi c}{2\pi f D(\varepsilon_r + 1)\ln\left[\csc\left(\frac{\pi g}{2D}\right)\right]}, \tag{10}$$

Figure 7 shows the total *RCS* of the single- and bi-layered mantel cloak. It can be seen that invisibility is obtained for a wide range of θ_i using the optimized values of the relative thickness a_d/a and spacer permittivity,

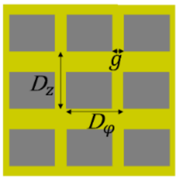

Figure 6. The rectangular-shaped metasurface coverings the PEC cylinder and its related parameters

TABLE 1. The calculated and refined optimal parameters for single- and bi-layered mantle cloaks

	Description	Param.	Values (mm)
PEC Cylinder	Cylinder radius	a	10
Single-layered structure	Spacer thickness	a_d	11
	Patch distance	g	1.5
	φ periodicity	D_φ	17.28
	z periodicity	D_z	24
bi-layered structure	First layer	a_{d1}	11.2
		g_1	1.2
		$D_{\varphi 1}$	17.28
		D_{z1}	12.6
	Second layer	a_{d2}	13
		g_2	1.2
		$D_{\varphi 2}$	8.64
		D_{z2}	12.1

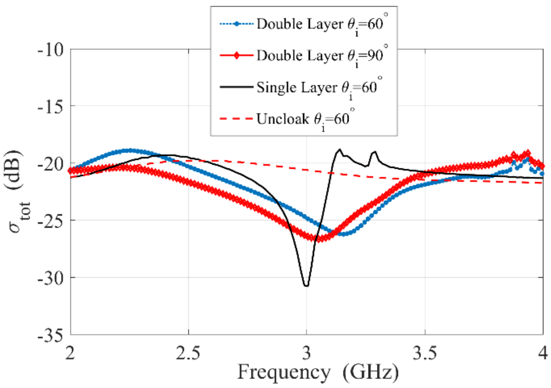

Figure 7. The total *RCS* for the single- and bi-layered mantel cloak versus frequency

resulting in acquiring the required surface impedance values using the rectangular-shaped metasurface. Notably, the frequency range in which the invisibility is achieved using the bi-layered structure is nearly doubled compared to that of the single-layered cloak. Figure 7 also confirms that, at 3 GHz, the bi-layered mantle cloak provides 1 GHz bandwidth, corresponding to a fractional bandwidth of 33%. So, the bi-layered metasurface can significantly reduce scattered fields over a wideband frequency range, interpreting the object as invisible. The photos of the electric field for the cloaked- and bared cylinder are shown in Figure 8, which confirms that the field distribution is strongly disturbed in the case of the cloaked cylinder. However, by covering the metallic cylinder using the designed metasurface, the wavefronts for the cloaked- and bared-cylinder is illustrated in Figure 8. It can be concluded that field distribution is powerfully disturbed in the case of the cloaked cylinder. However, by covering the metallic cylinder using the designed metasurface, the wavefronts rotate around the object leading to become invisible.

The simulated patterns of the total *RCS* for the cloaked and uncloaked cylinder are depicted in Figure 9 versus φ in the observation angle of $\theta_s = 120^\circ$, since the impinging angle is $\theta_i = 60^\circ$ which confirms that the designed bi-layered metasurface as mantle cloak significantly reduces the scattered fields. Also, it indicates that in all observation angles the cloak is efficient.

Table 2. summarizes a comparison between published works in the literature and the proposed technique in terms of cloaking performance and bandwidth. As can be seen, the introduced bi-layeedr rectangular patch metasurfaces with 33% bandwidth at 3 GHz provides better performance than the other published works wich represent the robustness of the

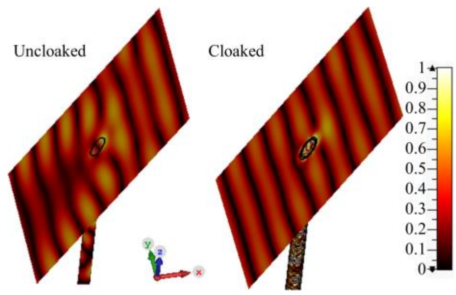

Figure 8. The snapshots of the normalized electric fields of the cloaked and uncloaked cylinder for $\theta_i = 60^\circ$

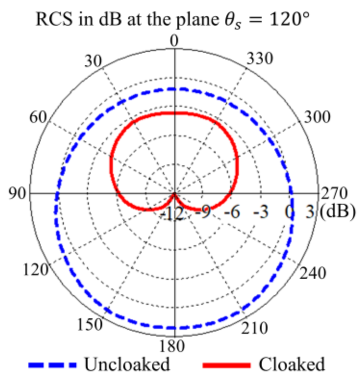

Figure 9. The simulated total *RCS* patterns of the bare and cloaked cylinder versus φ, for $\theta_i = 60^\circ$ and $\theta_s = 120^\circ$

TABLE 2. The comparsion of cloaking and bandwidth performaance with published works

Ref.	Metasurface	Frequncy (GHz)	Cloaking Perfomance (dB)	Cloaking BW (%)
[25]	Graphene Metasurface	4	5.2	30
[29]	Nonlinear Metasurface	3	30	10
[30]	Huygens' Metasurface	4	15	27.5
[31]	Metallic patches	9	6.2	16.6
[21]	Metallic patches	3	6	20
[32]	I-Shaped Metasurface	3	10	10
[18]	Metallic patches	3.3	8	30
This Work	Rectangular Patch	3	6	33

proposed methode to increase the cloaking bandwidth while an obliquely incident wave is impinged on a PEC cylinder.

4. CONCLUSION

This paper uses the established mantle cloak technique to study electromagnetic invisibility for a metallic cylinder illuminated by a broad range of obliquely incidence angles for both TM and TE waves. It is shown that the scattered fields provide co- and cross-polarized terms due to obliquely impinging waves. To settle the issue and consider these two components simultaneously, a metasurface sheet impedance is used, which is modeled by a tensor model for both waves. The metasurface is made by rectangular-patch, which provides capacitive reactance to diminish the scattered fields and significantly decrease the total *RCS* leading to hiding the object from the incoming wave. The systematic formulation is verified using numerical investigation by CST software. To widen the available bandwidth, a bi-layered mantle cloak is also designed, resulting in nearly 33% cloaking bandwidth, which is twice that of the single-layered mantle clock at 3 GHz for a PEC cylinder with a radius of 10 mm.

5. REFERENCES

1. Schurig, D., Mock, J.J., Justice, B., Cummer, S.A., Pendry, J.B., Starr, A.F. and Smith, D.R., "Metamaterial electromagnetic cloak at microwave frequencies", ***Science***, Vol. 314, No. 5801, (2006), 977-980, DOI: 10.1126/science.1133628.
2. Alù, A. and Engheta, N., "Achieving transparency with plasmonic and metamaterial coatings", ***Physical Review E***, Vol. 72, No. 1, (2005), 016623, DOI: 10.1103/ PhysRevE. 72.016623.
3. Alù, A. and Engheta, N., "Plasmonic cloaks", in Metamaterials and Plasmonics: Fundamentals, Modelling, Applications, Springer. (2009), 37-47, DOI: 10.1007/978-1-4020-9407-1_3.
4. Pendry, J. B., Schurig, D. and Smith, D. R., "Controlling electromagnetic fields", ***Science***, Vol. 312, No. 5781, (2006), 1780-1782, DOI: 10.1126/science.1125907 10.1126/science.1125907.
5. Leonhardt, U., "Optical conformal mapping", ***Science***, Vol. 312, No. 5781, (2006), 1777-1780, DOI: 10.1126/science.1126493.
6. Padooru, Y.R., Yakovlev, A.B., Chen, P.-Y. and Alu, A., "Analytical modeling of conformal mantle cloaks for cylindrical objects using sub-wavelength printed and slotted arrays", ***Journal of Applied Physics***, Vol. 112, No. 3, (2012), 034907, DOI: 10.1063/1.4745888.
7. Ergin, T., Stenger, N., Brenner, P., Pendry, J.B. and Wegener, M., "Three-dimensional invisibility cloak at optical wavelengths", ***Science***, Vol. 328, No. 5976, (2010), 337-339, DOI: 10.1126/science.1186351.
8. Valentine, J., Li, J., Zentgraf, T., Bartal, G. and Zhang, X., "An optical cloak made of dielectrics", ***Nature Materials***, Vol. 8, No. 7, (2009), 568-571, DOI: 10.1038/nmat2461.
9. Alù, A. and Engheta, N., "Cloaking a sensor", ***Physical Review letters***, Vol. 102, No. 23, (2009), 233901, DOI: 10.1103/PhysRevLett.102.233901.
10. Alù, A. and Engheta, N., "Multifrequency optical invisibility cloak with layered plasmonic shells", ***Physical Review Letters***, Vol. 100, No. 11, (2008), 113901, DOI: 10.1103/PhysRevLett.100.113901.
11. Alu, A. and Engheta, N., "Plasmonic and metamaterial cloaking: Physical mechanisms and potentials", ***Journal of Optics A: Pure and Applied Optics***, Vol. 10, No. 9, (2008), 093002, DOI: 10.1088/1464-4258/10/9/093002.
12. Milton, G.W. and Nicorovici, N.-A.P., "On the cloaking effects associated with anomalous localized resonance", ***Proceedings of the Royal Society A: Mathematical, Physical and Engineering Sciences***, Vol. 462, No. 2074, (2006), 3027-3059, DOI: 10.1098/rspa.2006.1715.
13. Yuste, P., Rius, J. M., Romeu, J., Blanch, S., Heldring, A. and Ubeda, E., "A microwave invisibility cloak: The design, simulation, and measurement of a simple and effective frequency-selective surface-based mantle cloak", ***IEEE Antennas and Propagation Magazine***, Vol. 60, No. 4, (2018), 49-59, DOI: 10.1109/MAP.2018.2839903.
14. Alù, A., "Mantle cloak: Invisibility induced by a surface", ***Physical Review B***, Vol. 80, No. 24, (2009), 245115.
15. Chen, P.-Y. and Alu, A., "Mantle cloaking using thin patterned metasurfaces", ***Physical Review B***, Vol. 84, No. 20, (2011), 205110, DOI: 10.1103/PhysRevB.80.245115.
16. Chen, P.-Y., Montione, F. and Alu, A., "Suppressing the electromagnetic scattering with a helical mantle cloak", ***IEEE Antennas and Wireless Propagation Letters***, Vol. 10, (2011), 1598-1601, DOI: 10.1109/LAWP. 2011. 2179001.
17. Monti, A., Toscano, A. and Bilotti, F., "Metasurface mantle cloak for antenna applications", in Proceedings of the 2012 IEEE International Symposium on Antennas and Propagation, IEEE. (2012), 1-2, DOI: 10.1109/APS.2012. 6348711.
18. Soric, J.C., Alù, A., Kerkhoff, A. and Rainwater, D., "Experimental demonstration of a conformal mantle cloak for radio-waves", in Proceedings of the 2012 IEEE International Symposium on Antennas and Propagation, IEEE. (2012), 1-2, DOI: 10.1109/APS.2012.6349400.

19. Monti, A., Bilotti, F., Toscano, A., Soric, J. and Alù, A., "Mantle cloak devices for TE and TM polarizations", in 2013 IEEE Antennas and Propagation Society International Symposium (APSURSI), IEEE. (2013), 324-325, DOI: 10.1109/APS.2013.6710823.

20. Bernety, H. M. and Yakovlev, A. B., "Metasurface cloaks for dielectric and metallic elliptical cylinders and strips", in 2014 International Conference on Electromagnetics in Advanced Applications (ICEAA), IEEE. (2014), 496-499, DOI: 10.1109/ICEAA.2014.6903905.

21. Moosaei, A. and Neshati, Mohammad H., "Design investigation of mantle-cloak for a PEC cylindrical object under oblique incidence of TM and TE waves", ***AEU-International Journal of Electronics and Communications***, Vol. 137, (2021), 153801, DOI: 10.1016/j.aeue.2021.153801.

22. Balanis, C., "Advanced engineering electromagnetics", John Wiley & Sons,, *NewYork*, 1989.

23. Moosaei, A. and Neshati, Mohammad H., "Wide-band cloaking of finite length pec cylindrical objects under oblique incidence using multi-layer mantle cloak", in 2021 29th Iranian Conference on Electrical Engineering (ICEE), IEEE. (2021), 886-890, DOI: 10.1109/ICEE52715.2021. 9544464.

24. Hamzavi-Zarghani, Z., Yahaghi, A. and Matekovits, L., "Electrically tunable mantle cloaking utilizing graphene metasurface for oblique incidence", ***AEU-International Journal of Electronics and Communications***, Vol. 116, (2020), 153080, DOI: 10.1016/j.aeue.2020.153080.

25. Pawar, S., Bernety, H.M. and Yakovlev, A.B., "Cloaking of cylindrical objects with graphene-metasurface structures for low-terahertz applications", in 2022 IEEE International Symposium on Antennas and Propagation and USNC-URSI Radio Science Meeting (AP-S/URSI), IEEE. (2022), 1366-1367, DOI: 10.1109/AP-S/USNC-URSI47032.2022. 9886308.

26. Bilotti, F., Tricarico, S. and Vegni, L., "Plasmonic metamaterial cloaking at optical frequencies", ***IEEE Transactions on Nanotechnology***, Vol. 9, No. 1, (2009), 55-61, DOI: 10.1109/TNANO.2009.2025945.

27. Studio, C.M., "CST microwave studio", ***CST Studio Suite***, (2020).

28. Osipov, A. V. and Tretyakov, S. A., "Modern electromagnetic scattering theory with applications", John Wiley & Sons, NewYork, 2017.

29. S. Vellucci et al., "On the use of nonlinear metasurfaces for circumventing fundamental limits of mantle cloaking for antennas," ***IEEE Transactions on Antennas and Propagation***, Vol. 69, No. 8, (2021), 5048-5053, DOI: 10.1109/TAP.2021.3061010.

30. H. Younesiraad, Z. Hamzavi-Zarghani, and L. Matekovits, "Invisibility utilizing Huygens' metasurface based on mantle cloak and scattering suppression phenomen," ***IEEE Transactions on Antennas and Propagation***, Vol. 69, No. 8, (2021), 5181-5186, DOI: 10.1109/TAP.2021.3060022.

31. V. Pratik, M. Singh Bisht, and K .Vaibhav Srivastava, "Improving performance of mantle cloak for electrically large PEC cylinders by reducing higher-order scattering coefficients," ***Journal of Electromagnetic Waves and Applications,*** Vol. 35, No. 9, (2021), 1176-1191, DOI: 10. 1080/09205071.2021.1872042.

32. M. Bisht, V. P. Vinubhai, and K. V. Srivastava, "Analysis and realization of a wideband mantle cloak with improved cloaking performance," ***Journal of Electromagnetic Waves and Applications***, Vol. 34, No. 10, (2020), 1386-1399, DOI: 10.1080/09205071.2020.1726213

Persian Abstract

چکیده

در این مقاله، فراابتکاری جدید Dhouib-Matrix-4 (DM4) برای بهینه‌سازی سیاست‌های تعمیر پوشش برای شبکه‌های حسگر بی‌سیم با استفاده از یک ربات متحرک با سرعت‌های متحرک متفاوت، بهبود می‌یابد. به صورت سلسله مراتبی، دو معیار متناقض در نظر گرفته می شود: ابتدا تعداد گره هایی که باید در زمان بازدید شوند به حداکثر می رسد، سپس در مرحله دوم، فاصله مسیر به حداقل می رسد. DM4 یک روش چند استارتی است که در هر شروع از اکتشافی حریصانه جدید Dhouib-Matrix-TSP1 استفاده می کند تا یک راه حل اولیه اولیه را ایجاد کند که توسط تکنیک جستجوی محلی جدید با عنوان Far-to-Near تشدید می شود. DM4 در هفت نمونه استاندارد از ادبیات استفاده می شود که در آن سرعت حرکت (w) یک بازیگر متحرک از ۰.٤ تا ۱ متغیر است. عملکرد DM4 با مقایسه نتایج آن با نتایج ایجاد شده توسط الگوریتم تکاملی (EA) که در آن DM4 عملکرد بهتری دارد اثبات می شود. EA در چهار نمونه و نتایج یکسانی را برای سه نمونه یادآوری می یابد. DM4 تحت زبان برنامه نویسی پایتون توسعه یافته است و یک نمایش گرافیکی از راه حل تولید شده نشان داده شده است.